Regional Seismic Wavefield Modeling with a Generalized Pseudospectral Method

Jeffrey Orrey and Charles Archambeau
Dept. of Physics, TAGG
University of Colorado
Boulder, CO 80309-0583

Contract No. F49620-94-1-0124

ABSTRACT

In this study we apply a numerical modeling method to predict and analyze discriminatory seismic signals in realistic models of the crust and to characterize wave propagation effects as functions of source and medium characteristics. The numerical method we use is the recently-developed generalized Fourier method (GFM). Based on the standard Fourier pseudospectral method, the generalized method exhibits optimal gridpoint-per-minimum-wavelength sampling and no numerical dispersion from spatial approximations. In addition, the highly accurate interface boundary condition approximations in GFM makes the method very useful for the study of the regional propagation of the discriminatory phase Lg and the effects of source and structure characteristics on the relative strengths of Lg and Rg, as well as crustal body wave phases. Furthermore, the method's computational efficiency, from the standpoint of machine storage requirements, makes possible relatively broadband simulations, relative to lower-order finite difference and finite element simulations, in both two and three dimensions.

Numerical simulations are performed to systematically determine the effects of random (small scale) and coherent (large scale) heterogeneities, anelasticity (without a weak attenuation limitation), and irregular layer topography on the energy partitioning between important seismic phases, such as Pg, Lg, and Rg. We find that Rg scattering to Lg is the dominant mechanism determining the relative amplitudes of these phases, and our results suggest the necessity of using fully-heterogeneous 3-D simulations to quantitatively assess the causes and effects of scattering in the crust.

Regional Seismic Wavefield Modeling with a Generalized Pseudospectral Method

Objective

In this study we apply a numerical modeling method to predict and analyze discriminatory seismic signals in realistic models of the crust and to characterize wave propagation effects as functions of source and medium characteristics. The numerical method we use is the recently-developed generalized Fourier method (Orrey [3], Orrey *et al.* [4]). Based on the standard Fourier pseudospectral method (Fornberg [2]), the generalized Fourier method (GFM) exhibits optimal gridpoint-per-minimum-wavelength sampling and no numerical dispersion from spatial approximations. In addition, the unusual accuracy of interface boundary condition approximations in GFM makes the method very useful for the study of the regional propagation of the discriminatory phase L_g and the effects of source and structure characteristics on the relative strengths of L_g and R_g, as well as crustal body wave phases. Furthermore, the method's computational efficiency, from the standpoint of machine storage requirements, makes possible relatively broadband simulations, relative to lower-order finite difference and finite element simulations, in both two and three dimensions.

The objective of this study is (1) to increase the bandwidth of current 2-D and 3-D wavefield simulations in complicated, laterally-varying earth structures, (2) to systematically determine the effects of random (small scale) and coherent (large scale) heterogeneities, anelasticity, and irregular layer topography on the energy partitioning of important discriminatory signals in the crust, and (3) to quantitatively characterize discriminant dependence on differences in seismic sources, such as those from earthquakes of various types, tamped and decoupled nuclear explosions, and large industrial explosions.

Research Accomplished

A series of GFM wavefield simulations were performed for 2-D Earth models which contain complexities typical of the Earth's crust. The examples given illustrate the method's capabilities for studies of the effects of medium complexity on seismic signals and suggest directions of further study for simulations in media with three-dimensional variations in structure. All of the complicated Earth models considered in this paper are obtained by increasing the complexity of a layered crustal model containing nine layers. We examine the

wavefield propagation effects of randomization, attenuation and coherent lateral variations of this structure.

The first structural complexity we consider is the addition of random variations to the velocity values of the layered structure. In this regard, Figure 1 illustrates the effects of random spatial variations in the velocity values about mean values within a layered model, where the randomization is in both the vertical and lateral directions. In particular, Figure 1(a) shows the GPM synthetic seismograms for an explosion at 1 km depth in a layered crustal model with nine layers, and Figure 1(b) shows the seismograms in the same model with 10% rms variability imposed on the (mean) P and S wave velocities. Clearly there are major differences, in that the R_g phase is reduced as a function of distance from the source and the L_g and P_g phases are considerably increased and more complex. Since this effect is generally observed, we conclude that random fluctuations are responsible for the relatively large L_g observed relative to R_g at greater distances from the source. In this case the L_g energy is largely derived from scattering from R_g, with an associated rapid attenuation of R_g with distance and a relative growth of L_g amplitudes.

Figure 2(a), again for an explosion source at 1 km depth and a lateral position of 30 km, shows the effects of vertically and laterally discontinuous changes in the randomization, where the rms percentage of randomization changes from layer to layer in depth (with decreasing fluctuations with depth) and also decreases within lateral zones at greater distances from the explosion source. The randomization model is given in Table 1. For this model, the

Table 1: Randomization model used for the simulations of Figures 2(a) and 2(b). Each zone is 100 km in lateral extent.

depth range (km)	rms fluctuations (%)			
	zone 1	zone 2	zone 3	zone 4
$0 \le z \le 5$	25	20	15	10
$5 < z \le 10$	20	15	10	5
$10 < z \le 15$	15	11	7	3
$15 < z \le 30$	10	7	5	3
$30 < z$	5	4	3	3

L_g is larger and the R_g smaller than was the case for the results in Figure 1(b), which had the same average velocity values. This change is largely due to the larger fluctuations in near-surface P and S velocities for the model used for Figure 2(a) compared to the structure model for Figure 1(b) (25% compared to 10% in the upper 1 km near the source). These large random velocity variations, of 25% and greater, are commonly observed from well logs and can persist to depths of at least 5 km in most areas. Therefore, the structure model used in Figure 2(a) is not extreme and, indeed, is probably conservative with respect to velocity fluctuations, particularly in tectonic areas. Furthermore, the synthetic seismograms in 2(a) are yet closer approximations to those commonly observed, compared to those in Figure 1(b).

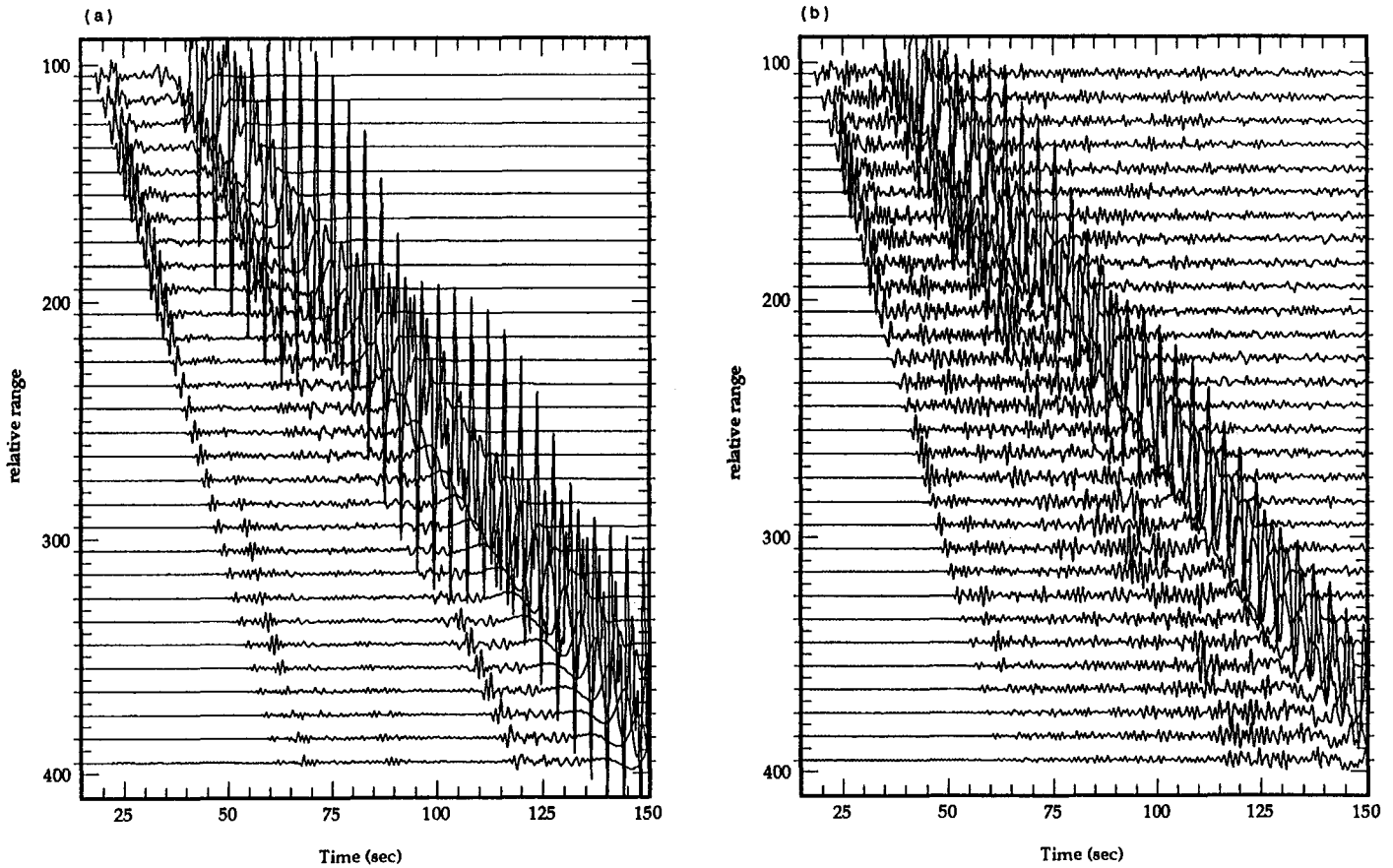

Figure 1: Comparison of GFM generated seismograms at different regional distances (in km) from an explosive source at 1 km depth in (a) the layered crustal structure and (b) the layered structure with 10 % random fluctuations in the elastic velocities. No anelastic attenuation was included in either simulation. Note in (b) the much lower levels of the R_g surface wave at larger distances and the larger amplitudes of P_g and L_g relative to the results in (a), showing the transfer of energy from the fundamental mode (R_g) to the higher modes making up P_g and L_g. This effect increases as random fluctuations increase in magnitude.

Figure 2(b) shows seismograms for a simple double couple source at a depth of 5 km in the same structure model used in Figure 2(a). In this simulation, the short period R_g excitation is lower, relative to the explosion in (5a), in part due to its greater source depth. and the P, P_g and L_g waves are also different for the two source types. However, in order to quantify the relative differences, it will be necessary to account for radiation pattern effects in a full 3-D, azimuthally-variable simulation.

Figures 3(a) and 3(b) show the effects of anelastic attenuation when compared to the simulations in Figure 2(a). In particular, the structure and explosive source used for the elastic simulation in 2(a) are also used for the simulations in Figures 3(a) and 3(b). However, in the latter simulations anelastic effects were included by the introduction of a space-dependent Q using the attenuation method of Emmerich and Korn [1]. Thus the results in Figure 2(a) are for an elastic medium (infinite Q), while those in Figures 3(a) and 3(b) include different levels of dissipation. The results in Figure 3(a) were produced with a depth-dependent Q, with a Q value of 150 near the free surface and increasing Q with depth, while those in Figure 3(b) are for a (low) Q value of 25 near the surface that also increases with depth. Comparing Figures 2(a) and 3(a) indicates a modest decrease in R_g and L_g due to moderate anelastic attenuation, while comparison of the results for the low Q case in Figure 3(b) with the elastic or moderate Q cases shows a dramatic reduction in both the R_g and L_g energy with distance while the P waves remain relatively unaffected. We note that a low near-surface Q model will always have a rather drastic effect on the short period R_g and L_g surface wave modes and that in comparison to actual data this is not typically the case. That is, while R_g decreases rapidly with distance, L_g does not, and in fact the L_g coda tends to increase in duration and magnitude in many areas. This suggests that R_g scattering to L_g is the dominant mechanism and that results like those in Figure 3(a), with a moderate Q, are appropriate in the general case.

In the final example, we show the effect on crustal phases of the large-scale lateral variation in structure illustrated in Figure 4. This structure is intended to approximate the occurrence of a sedimentary basin along the source-receiver path. Figure 5 shows the seismograms obtained from a simulation through the structure of Figure 4. These results should be compared to those in Figure 2(a) since the model used contained no anelastic dissipation and the velocity structure was the same for both simulations, except for the presence of the basin in the results in Figure 5. Clearly the R_g phase is strongly affected by the basin structure, with reduced amplitudes upon emergence from the basin, and the L_g is also reduced. Thus, this large-scale structure had the effect of "blocking" both R_g and L_g while not affecting the P and P_g phases very much.

Conclusions

To some extent, even with the small sampling of simulations presented here, it is possible to infer specific effects of structure variations on the important discriminatory signals. These examples suggest the similarity of the results of the numerical simulations to observed seismograms. Realistic synthetic data can be analyzed in precisely the way field observations would be analyzed to form various discriminatory measures (e.g. modified m_b vs. M_s at

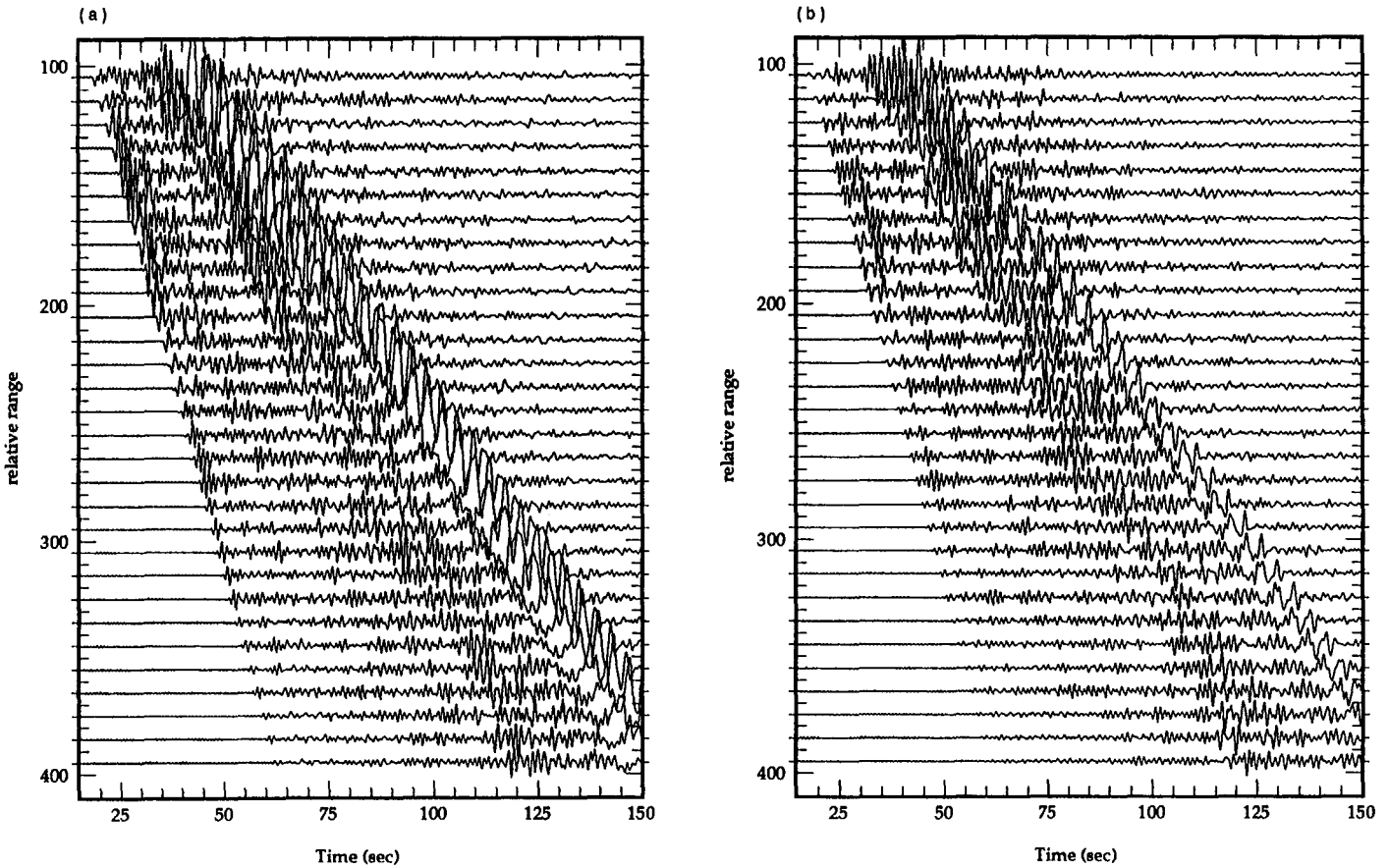

Figure 2: GFM generated seismograms in the layered structure with strong, random elastic velocity fluctuations and no anelastic attenuation. The strongest fluctuations are 25 % rms, and the fluctuations decrease with distance from the source. The source in (a) was an explosion at 1 km depth, and the source in (b) was a double couple at a depth of 5 km with the fault plane oriented at 45 degrees from the vertical.

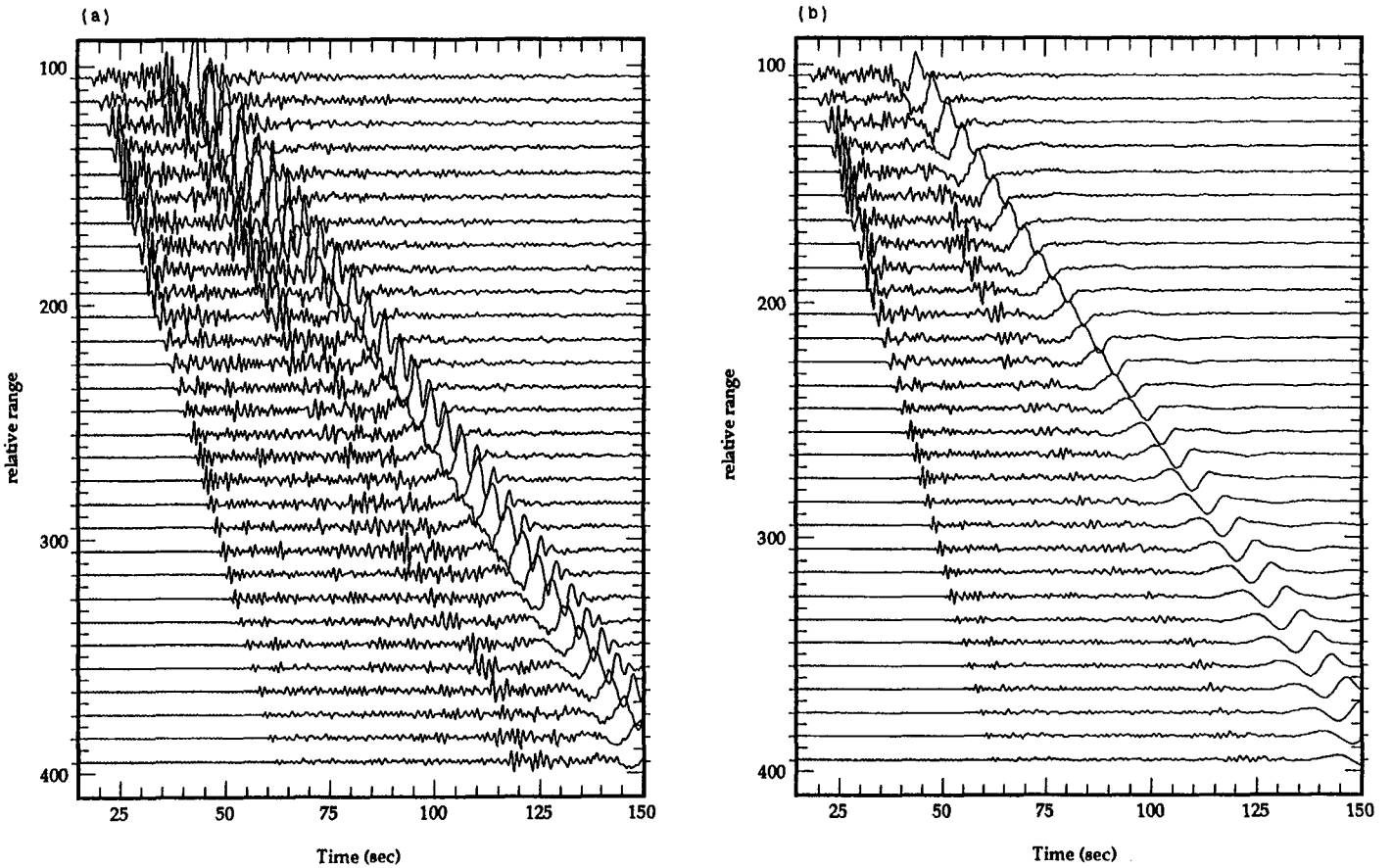

Figure 3: GFM generated seismograms in the same structure used for the simulations of Figure 2 except these models contain anelastic dissipation effects. The Q values are depth-dependent, with the Q increasing with depth. In (a), the minimum Q value is 150 near the free surface. In (b), the Q values are much lower, with a minimum Q value of 25 near the free surface.

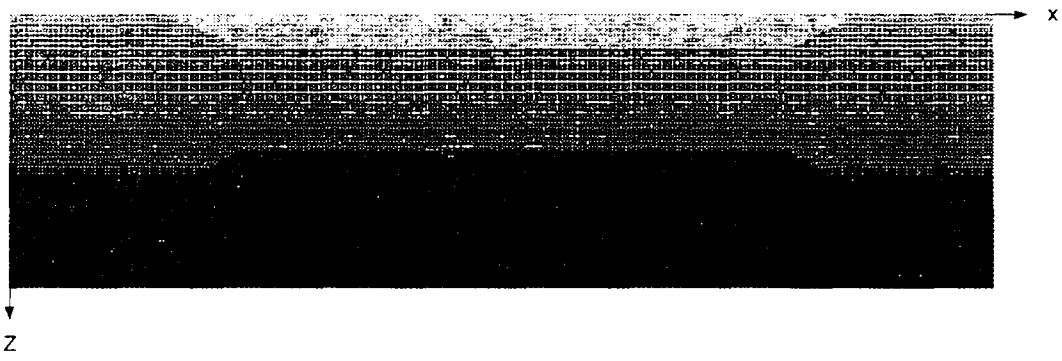

Figure 4: Randomized basin structure used to generate the seismograms in Figure 5. Light shades indicate low velocities and dark shades indicate high velocities. The basin and its associated mantle uplift span a source-receiver range (x) of 70 km to 270 km, and the basin extends to a depth (z) of 10 km and contains stronger (30 % rms) near-surface velocity fluctuations than exist in the surrounding structure.

different frequencies, spectral ratios, etc.) in order to infer their physical basis, robustness, variability and any structure-induced anomalies.

References

[1] H. Emmerich and M. Korn. Incorporation of attenuation into time-domain computations of seismic wave fields. *Geophysics*, 52(9):1252–1264, September 1987.

[2] B. Fornberg. The pseudospectral method: Comparisons with finite differences for the elastic wave equation. *Geophysics*, 52(4):483–501, April 1987.

[3] J. L. Orrey. *A Generalized Fourier Pseudospectral Method for Elastodynamics.* PhD thesis, University of Colorado, Boulder, 1995.

[4] J. L. Orrey, C. B. Archambeau, and G. A. Frazier. Complete elastic wavefield synthesis with a pseudospectral method: The Generalized Fourier Method. Submitted to *Geophys. J. Int.*

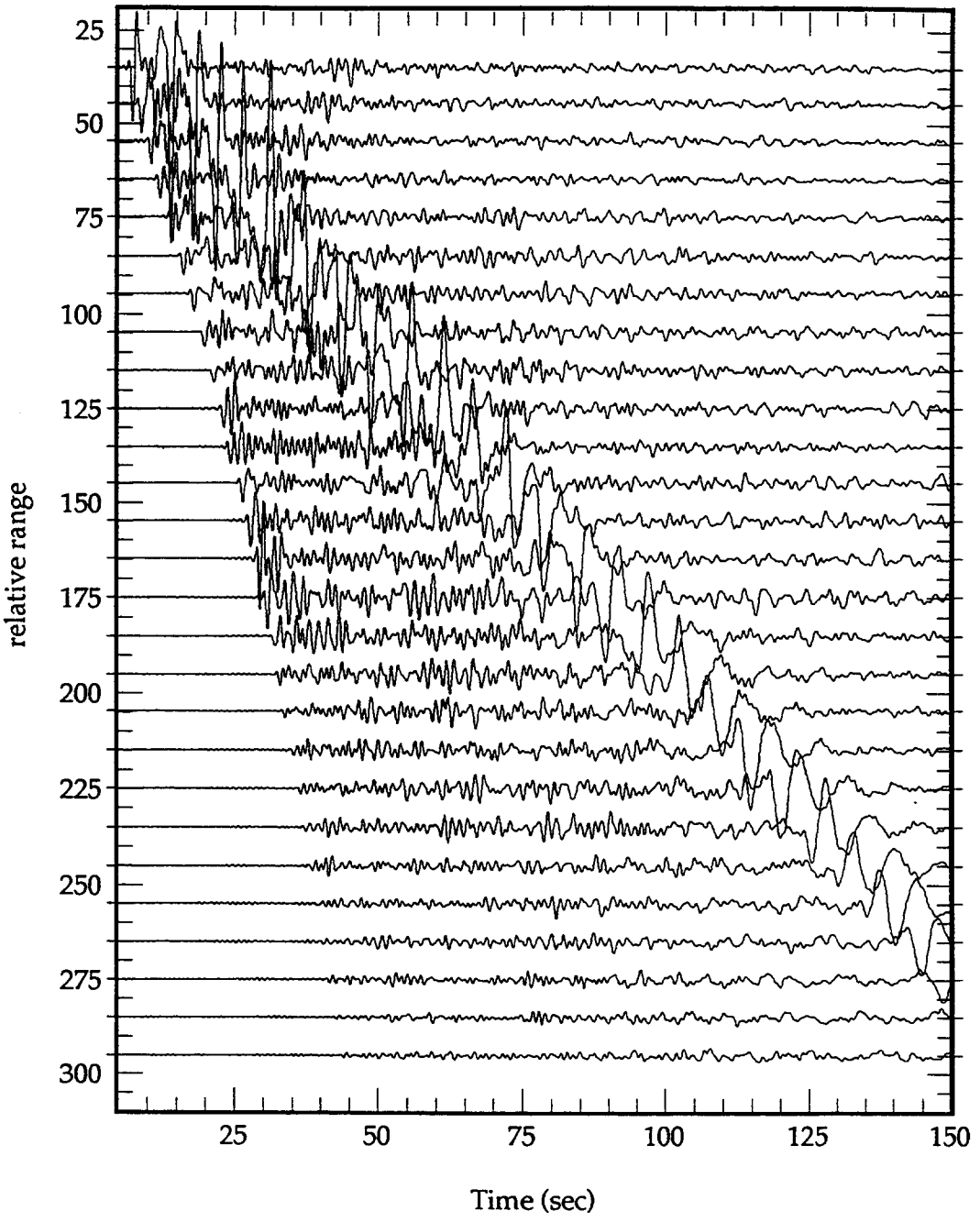

Figure 5: GFM generated seismograms from an explosive source at 1 km depth in the layered, randomized basin structure of Figure 4.